Precision Medicine and Imaging

Validation of Microsatellite Instability Detection Using a Comprehensive Plasma-Based Genotyping Panel

Jason Willis[1], Martina I. Lefterova[2], Alexander Artyomenko[2], Pashtoon Murtaza Kasi[3], Yoshiaki Nakamura[4], Kabir Mody[5], Daniel V.T. Catenacci[6], Marwan Fakih[7], Catalin Barbacioru[2], Jing Zhao[2], Marcin Sikora[2], Stephen R. Fairclough[2], Hyuk Lee[8], Kyoung-Mee Kim[9], Seung Tae Kim[10], Jinchul Kim[10], Danielle Gavino[11], Manuel Benavides[12], Nir Peled[13], Timmy Nguyen[14], Mike Cusnir[15], Ramez N. Eskander[16], Georges Azzi[17], Takayuki Yoshino[18], Kimberly C. Banks[2], Victoria M. Raymond[2], Richard B. Lanman[2], Darya I. Chudova[2], AmirAli Talasaz[2], Scott Kopetz[1], Jeeyun Lee[10], and Justin I. Odegaard[2]

Abstract

Purpose: To analytically and clinically validate microsatellite instability (MSI) detection using cell-free DNA (cfDNA) sequencing.

Experimental Design: Pan-cancer MSI detection using Guardant360 was analytically validated according to established guidelines and clinically validated using 1,145 cfDNA samples for which tissue MSI status based on standard-of-care tissue testing was available. The landscape of cfDNA-based MSI across solid tumor types was investigated in a cohort of 28,459 clinical plasma samples. Clinical outcomes for 16 patients with cfDNA MSI-H gastric cancer treated with immunotherapy were evaluated.

Results: cfDNA MSI evaluation was shown to have high specificity, precision, and sensitivity, with a limit of detection of 0.1% tumor content. In evaluable patients, cfDNA testing accurately detected 87% (71/82) of tissue MSI-H and 99.5% of tissue microsatellite stable (863/867) for an overall accuracy of 98.4% (934/949) and a positive predictive value of 95% (71/75). Concordance of cfDNA MSI with tissue PCR and next-generation sequencing was significantly higher than IHC. Prevalence of cfDNA MSI for major cancer types was consistent with those reported for tissue. Finally, robust clinical activity of immunotherapy treatment was seen in patients with advanced gastric cancer positive for MSI by cfDNA, with 63% (10/16) of patients achieving complete or partial remission with sustained clinical benefit.

Conclusions: cfDNA-based MSI detection using Guardant360 is highly concordant with tissue-based testing, enabling highly accurate detection of MSI status concurrent with comprehensive genomic profiling and expanding access to immunotherapy for patients with advanced cancer for whom current testing practices are inadequate.

Introduction

Microsatellite instability (MSI) is a National Comprehensive Cancer Network (NCCN) clinical practice guidelines-recommended biomarker in at least nine cancer types—cervical, cholangiocarcinoma, colorectal, endometrial, esophageal and esophagogastric, gastric, ovarian, pancreatic, and prostate cancers (1–9)—due to its importance as a predictive biomarker for response to immune checkpoint blockade (ICB) as exemplified by pan-cancer approval of pembrolizumab (10, 11). Detection of MSI in a patient with advanced cancer can also alert the clinician to evaluate the patient's asymptomatic family members for hereditary cancer risk.

[1]The University of Texas MD Anderson Cancer Center, Houston, Texas. [2]Guardant Health, Redwood City, California. [3]Division of Oncology/Hematology, Department of Internal Medicine, University of Iowa, Iowa City, Iowa. [4]Department of Gastroenterology and Gastrointestinal Oncology, National Cancer Center Hospital East, Kashiwa, Japan. [5]Division of Hematology and Medical Oncology, Mayo Clinic, Jacksonville, Florida. [6]Department of Medicine, University of Chicago, Chicago, Illinois. [7]Medical Oncology, City of Hope, Duarte, California. [8]Division of Gastroenterology, Samsung Medical Center, Sungkyunkwan University School of Medicine, Seoul, Republic of Korea. [9]Division of Pathology, Samsung Medical Center, Sungkyunkwan University School of Medicine, Seoul, Republic of Korea. [10]Division of Hematology-Oncology, Samsung Medical Center, Sungkyunkwan University School of Medicine, Seoul, Republic of Korea. [11]INVITAE Corporation, San Francisco, California. [12]Medical Oncology, Hospital Universitario Virgen de la Victoria, Malaga, Spain. [13]Division of Medical Oncology, Rabin Medical Center, Petach Tiqea, Israel. [14]Hematology/Oncology, Cleveland Clinic Foundation, Weston, Florida. [15]Comprehensive Cancer Center, Mount Sinai Medical Center, Miami Beach, Florida. [16]Center for Personalized Cancer Therapy, Division of Gynecologic Oncology, University of California San Diego Health Moores Cancer Center, La Jolla, California. [17]Medical Oncology, Holy Cross Michael & Dianne Bienes Comprehensive Cancer Center, Fort Lauderdale, Florida. [18]Department of Gastroenterology and Gastrointestinal Oncology, National Cancer Center Hospital East, Kashiwa, Japan.

AACR OF1

Translational Relevance

Microsatellite instability (MSI) is an important biomarker predictive of response to immune checkpoint blockade (ICB) across solid cancers and may herald the presence of a hereditary cancer predisposition syndrome. However, despite being recommended by clinical practice guidelines, MSI is most often not assessed, in part due to tissue insufficiency, unavailability, or infeasibility. Noninvasive blood-based methods have been developed to detect MSI; however, these approaches are challenged by limited sensitivity. Here, we report the validation of a highly sensitive cell-free DNA (cfDNA) sequencing-based method that allows simultaneous guideline-comprehensive determination of MSI status and genomic biomarkers for all solid cancers. We further validate the clinical relevance of cfDNA-based MSI detection by reporting robust clinical activity of ICB therapy in 16 patients with cfDNA MSI-H gastric cancer.

MSI is the manifestation of defective DNA mismatch repair (dMMR), which leads to dramatically increased mutation rates throughout the genome, including gain and/or loss of nucleotides within repeating motifs known as microsatellite tracts, from which the entity derives its name. MSI is most prevalent in endometrial, colorectal, and gastroesophageal cancers, where it can be a sequela of sporadic mutations in MMR-related genes or a manifestation of Lynch syndrome, a hereditary cancer predisposition syndrome most commonly caused by germline mutations in *MLH1*, *MSH2*, *MSH6*, *PMS2*, or *EPCAM* (12). However, despite an increased prevalence in these cancer types, landscape analyses have shown that MSI also occurs at nonnegligible rates in most other solid tumors, including common tumor types such as lung, prostate, and breast cancer (13).

Recent studies have shown that MSI predicts clinical benefit from ICB with PD-1/PD-L1 inhibitors, which has led to the approval of these agents in several indications when MSI is present, including nivolumab ± ipilimumab for MSI-High (MSI-H, positive for MSI) metastatic colorectal cancer and pembrolizumab for unresectable or metastatic MSI-H solid tumors following progression on prior approved therapies (14). In addition to its value as a predictive biomarker for ICB benefit, MSI also has prognostic significance, most notably in colorectal cancer, where testing is recommended in clinical practice guidelines for all patients (3, 15).

Currently, MSI testing is most commonly performed via PCR and/or IHC analysis of tumor tissue specimens. The former assesses five canonical microsatellite loci originally recommended by the Bethesda panel (16, 17) and compares their length in tumor DNA relative to the germline genotype assessed in matched nontumor DNA; instability in the length of each microsatellite tract is used as direct evidence of MSI. However, this limited microsatellite panel was developed primarily for colorectal cancer and has more limited sensitivity in other cancer types (18). IHC approaches, in contrast, assess levels of four MMR proteins, with absence of expression of one or more (deficient MMR, dMMR) strongly correlated with MSI status. However, about 5% to 11% of MSI-H cases demonstrate intact MMR staining and localization (proficient MMR, pMMR) due to retained antigenicity and intracellular trafficking of an otherwise nonfunctional protein (19). Recent publications (20, 21) have

demonstrated that next-generation sequencing (NGS) can also accurately characterize MSI status in tumors, allowing for comprehensive profiling of targetable genomic biomarkers as well as MSI status via a single NGS test.

Despite recommendations across many cancer types in NCCN guidelines and associated FDA-approved treatment options, current rates of MSI testing outside of colorectal cancer and gastroesophageal carcinoma remain largely unknown. Even in colorectal cancer, where MSI testing recommendations have been in place since 2005 (17, 22), fewer than 50% of patients are tested (23), which results in missed ICB treatment opportunities and failure to recognize patients whose family members may be at increased risk for cancer. While multifactorial, such MSI undergenotyping is, in part, due to barriers associated with tissue acquisition, including difficulties locating archival diagnostic specimens or delays due to biopsy scheduling to obtain new tissue. In addition, invasive tissue acquisition procedures may be contraindicated in many heavily pretreated and/or frail patients and have the associated disadvantages of higher cost and procedural risk. Furthermore, the rapidly growing number of biomarkers and diversification of testing options creates daunting complexity for already overburdened physicians.

Cell-free circulating-tumor DNA (ctDNA) assays ("liquid biopsies") have successfully addressed such barriers in many genotyping indications by enabling minimally invasive profiling of contemporaneous tumor DNA. Liquid biopsies thus expand patient access to standard-of-care–targeted therapies, including ICBs, by identifying patients whose tumors harbor biomarkers of interest not otherwise identifiable due to tissue sampling limitations and do so more rapidly than typical tissue testing (24). Moreover, comprehensive liquid biopsies can provide all guideline-recommended somatic genomic biomarker information for all adult solid tumors in a single test.

In this study, we sought to enhance the utility of a previously validated ctDNA-based genotyping test through the addition of MSI detection. Here, we describe the design and validation of MSI assessment on this platform, report its performance on the largest ctDNA-tissue MSI validation cohort yet described ($n = 1{,}145$) and evaluate response prediction in 16 patients with advanced gastric cancer treated with ICB. We also report the MSI-H landscape more than 28,000 consecutive solid tumor patient samples tested in our Clinical Laboratory Improvement Amendment (CLIA)-certified, College of American Pathologists (CAP)-accredited, New York State Department of Health-approved laboratory.

Materials and Methods

Microsatellite loci selection

The Guardant360 test is a 74-gene panel previously validated for detection of SNVs, indels, CNAs, and fusions in all guideline-recommended indications for advanced solid tumors (25, 26). The assay initially incorporated 99 putative microsatellite loci consisting of short-tandem repeats of length 7 or more, which were selected to include sites susceptible to instability across multiple tumor types, including three of the five Bethesda panel sites (BAT-25, BAT-26, and NR-21). The remaining two Bethesda sites (NR-24 and MONO-27) were not included because of extremely low mappability of the regions. Coverage and noise profiles at these sites were assessed using sequencing data from a set of 84 healthy donor samples, to exclude uninformative sites from the final MSI detection algorithm.

Model description

MSI detection is based on integrating observed read sequences with molecular barcoding information into a single probabilistic model that compares the likelihood of observed data under PCR and sequencing noise assumptions with that under somatic MSI assumption. Each individual site with sufficient coverage is scored independently using Akaike Information Criterion (AIC; ref. 27), which is a statistical method for estimating the relative validity of different models describing how a given dataset was generated. The AIC model generates a locus score (ranging from 0 to infinity), reflecting the likelihood that observed variability at any given microsatellite locus is due to biological instability versus noise, and a locus is considered unstable if its score is above a trained threshold. The number of affected loci is calculated across the final 90 sites and the sample is called positive if the number of unstable loci (the "MSI Score") is above a trained threshold ($n = 6$). The thresholds for individual loci and total MSI score per sample were established using permutation-based simulations with data from healthy donor samples varying the frequencies of molecules with different repeat lengths and the error parameters at individual loci, as well as the overall number of unstable loci within a simulated sample. Through this approach, simulations were used to interrogate 100,000 combinations of microsatellite lengths and unstable locus numbers, which allows assessment of a diverse landscape of scenarios, some of which may not be represented in a nonsimulated dataset. The algorithm does not distinguish between microsatellite stable (MSS) and MSI-Low (a category defined by the observation of a single unstable Bethesda locus using PCR methods), grouping them into a single category. This is based on previous reports that MSI-L status is not a distinct phenotype but an artifact of testing a small number of microsatellites, such that when a large number of microsatellite loci are tested, previously characterized MSI-L samples mimic the MSS phenotype in overall MSI burden (28).

Samples

MSI algorithm development and training was performed using simulated data as well as a set of 84 healthy donor samples. The clinical validation study included 1,145 archived samples [residual plasma and/or cell-free DNA (cfDNA)] collected and processed as part of routine standard-of-care clinical testing in the Guardant Health CLIA laboratory as described previously (25), or archival patient plasma samples collected in EDTA blood collection tubes. Twenty healthy donor samples were also used for the analytical specificity study. Contrived samples used in the analytical validation studies comprise cfDNA pools extracted from cell line supernatants and healthy donor plasma. cfDNA was prepared from culture supernatants as described previously (25) using the following cell lines (ATCC, Inc.): KM12, NCI-H660, HCC1419, NCI-H2228, NCI-H1650, NCI-H1648, NCI-H1975, NCI-H1993, NCI-H596, HCC78, GM12878, MCF-7. cfDNA isolated from cell line culture supernatant mimics the fragment size and mechanisms of extracellular release (29), library conversion, and sequencing properties of patient-derived cfDNA, while also providing a renewable source of well-defined material of sufficient quantity to support the high material demands of studies such as limit of detection and precision.

Sample processing and bioinformatics analysis

cfDNA was extracted from plasma samples or cell line supernatants (QIAmp Circulating Nucleic Acid Kit, Qiagen, Inc.), and up to 30 ng of extracted cfDNA was labeled with nonrandom oligonucleotide barcodes (IDT, Inc.), followed by library preparation, hybrid capture enrichment (Agilent Technologies, Inc.), and sequencing by paired-end synthesis (NextSeq 500/550 or HiSeq 2500, Illumina, Inc.) as described previously. Bioinformatics analysis and variant detection were performed as described previously (25).

Analytical validation approach

The studies performed for analytical validation were based on established CLIA, Nex-StoCT Working Group, and Association of Molecular Pathologists/CAP guidance regarding performance characteristics and validation principles. To determine the sensitivity of the assay for MSI status, cfDNA from cell line supernatant from an MSI-H cell line derived from a patient with human colon cancer (KM12; ref. 30) was diluted with cfDNA from a MSS cell line (NCI-H660; refs. 31, 32) and tested at both standard (30 ng) and low (5 ng) cfDNA inputs. The dilution series targeted maximal variant allele fractions (max VAF) of 0.03%–2% for 5-ng input, and 0.01%–1% for 30-ng input. Targeted tumor fractions were verified using known germline variants unique to the titrant and diluent materials. Assessment of repeatability (within-run precision) and reproducibility (between-run precision) was based on clinical and contrived model samples. Six of the clinical samples for precision (three MSI-H, and three MSS) were selected with max VAF values of 1%–2%, representing approximately two to three times the predicted limit of detection (LoD) at 5 ng. MSI analytical specificity was determined by analyzing 20 healthy donor samples and 245 known MSS-contrived samples.

Clinical validation approach

Archived plasma or cfDNA from clinical samples from patients with available results from standard-of-care tissue-based MSI testing were tested using the ctDNA MSI algorithm ($n = 1,145$). Tissue-based MSI status was derived from IHC, PCR, or, less commonly, NGS. Clinical outcome data were extracted from patient medical records and deidentified by the treating physician.

Landscape analysis of plasma MSI status from 28,459 advanced cancer patient samples

The cohort comprised 28,459 consecutive advanced cancer patient samples tested using Guardant360 in the course of clinical care. All analyses were conducted with deidentified data and according to an IRB-approved protocol. The prevalence of MSI-H in this cohort was assessed across 16 primary tumor types: bladder carcinoma, breast carcinoma, cholangiocarcinoma, colon adenocarcinoma, cancer of unknown primary, head and neck squamous cell carcinoma, hepatocellular carcinoma, lung adenocarcinoma, lung cancer not otherwise specified, lung squamous cell carcinoma, "other" cancer diagnosis, pancreatic adenocarcinoma, prostate adenocarcinoma, stomach adenocarcinoma, and uterine endometrial carcinoma.

Statistical analysis

Statistical analyses were performed using Student t test for analysis of number of variants per sample and Fisher exact test for comparison of proportions. The lower and upper limits of the 95% confidence intervals (CI) for binomial proportions were calculated using Wilson score interval with continuity correction.

Ethics

This research was conducted utilizing deidentified data as per a protocol approved by the Quorum Institutional Review Board.

Willis et al.

Results

MSI algorithm development

Traditional challenges for ctDNA genotyping using NGS include efficient molecule capture due to low inputs and low tumor fraction in circulation (25, 26) and correction of sequencing and other technical artifacts. MSI detection presents additional challenges due to the need for (i) efficient molecular capture, sequencing, and mapping of repetitive genomic regions that accurately reflect MSI status; (ii) error correction and variant detection within repetitive regions; and (iii) differentiation of signal due to MSI from non-MSI somatic variation and the strong PCR slippage artifacts at sites typically impacted by somatic instability. Indeed, technical PCR error is typically at least an order of magnitude higher than typical sequencing error rates in homopolymeric sites, necessitating iterative site selection and optimal use of molecular barcoding to achieve relevant signal-to-noise detection ratios across a large number of candidate microsatellite sites.

While tissue sequencing panels often comprise sufficient informative microsatellite loci simply due to large panel size and longer DNA fragment lengths (13, 32), the moderate size of the ctDNA panel utilized here and short cfDNA fragment lengths require purposeful microsatellite selection and inclusion. To accomplish this, we used an iterative approach informed by literature and tissue sequencing compendia to evaluate candidate sites to provide pan-cancer MSI detection with minimal background noise. The list of candidate loci was further refined on the basis of the performance criteria referenced above using healthy donor cfDNA.

On the basis of the performance assessment in training healthy donor samples, informative loci were defined as those that were effectively captured, sequenced, and mapped and were associated with little variation within MSS samples (shown in gray in Fig. 1A). Uninformative loci either failed capture, sequencing, or mapping, resulting in inadequate molecular representation (shown in blue in Fig. 1A), or demonstrated substantial variation within MSS samples, resulting in excessive artifactual signal (shown in red in Fig. 1A). Interestingly, the *BAT-25*, *BAT-26*, and *NR-21* Bethesda loci utilized in traditional MSI tissue tests (16, 17) and some ctDNA panels (34) performed poorly relative to other candidates and were excluded from the final marker set (indicated by arrows in Fig. 1A).

Using this approach, 90 microsatellite loci were selected for inclusion in the final test version: 89 mononucleotide repeats and a single trinucleotide repeat, all of which comprise repeats of length 7 or above. Assessment of unique molecule coverage distribution demonstrated that 65% of these loci have coverage above $0.5\times$ median sample coverage.

In addition to effective molecular capture and mapping, MSI detection also requires highly accurate differentiation of cancer-related signal from background noise due to sequencing and polymerase errors at the very low allele fractions at which ctDNA is typically found (25, 26, 34). Importantly, the same repetitive genomic context that makes microsatellite candidates informative for MSI detection due to polymerase slippage during *in vivo* cellular replication also makes them particularly susceptible to the same polymerase slippage during *in vitro* library preparation and sequencing, resulting in high levels of technical noise. To address this, Digital Sequencing error correction was used to define true biological insertion–deletion events at microsatellite loci at high fidelity as
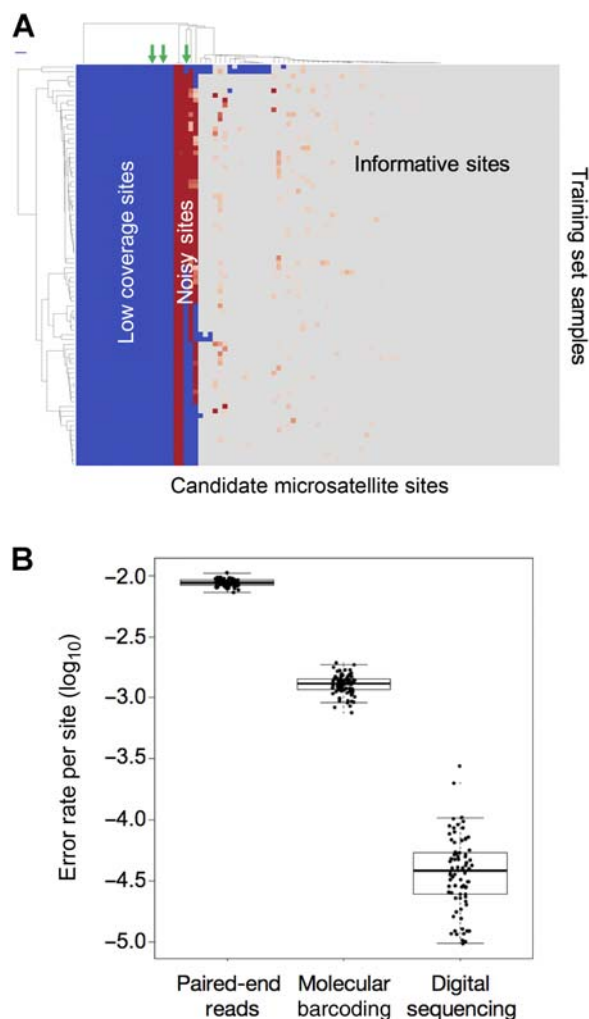

Figure 1.

Technical features of microsatellite detection. **A,** Hierarchical clustering of Aikake Information Criterion scores for 99 candidate microsatellite loci from cfDNA sequencing results from 84 healthy donors. Loci with poor unique molecule coverage are shown in blue, while loci with excessive technical artifact are shown in red. Robust but consistent measurements of microsatellite repeat length, as define an informative site, are shown in gray. Arrows indicate three Bethesda loci included in this study. **B,** Observed error rate reduction associated with each component of Digital Sequencing.

described previously (25, 26). Among these high background error repeats, Digital Sequencing was associated with 100-fold reduction in per-molecule sequencing error relative to standard sequencing approaches (Fig. 1B), allowing efficient and accurate reconstruction of microsatellite sequences of individual unique molecules present in the original patient blood sample. Site-specific and aggregate sample-level MSI status determination thresholds were then established using permutation-based threshold simulations of healthy donor samples. When these per-site and per-sample thresholds were combined with the effects of digital sequencing correction, the per-sample false positive rate was estimated to be approximately $10^{-7.3}$. In addition, titration simulations adjusted for the distribution of clinical inputs predicted robust MSI detection to approximately 0.2% tumor fraction, with a marked decline
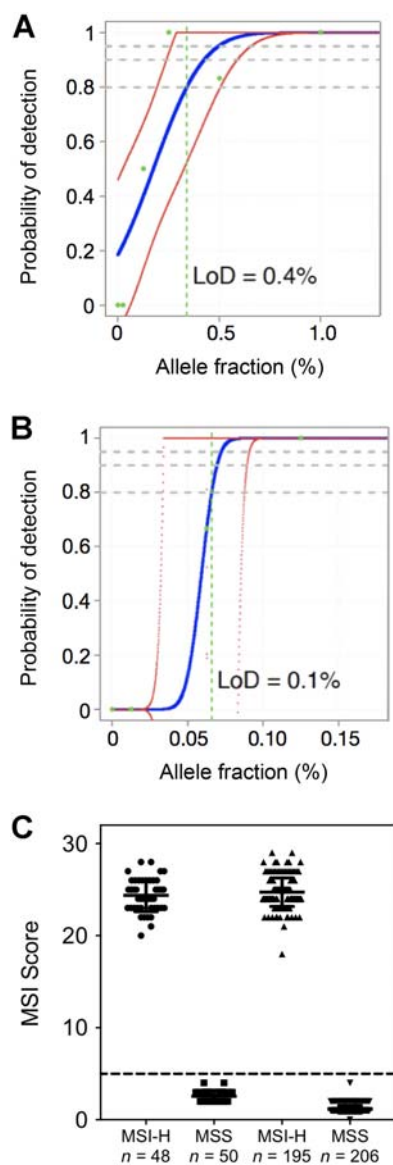
Figure 2.
Analytic validation of ctDNA MSI detection. Observed MSI detection rate was plotted by titration level (green dots), and probit regression was used to determine the 95% limit of detection for 5-ng (**A**) and 30-ng (**B**) cfDNA inputs. **C,** Sample-level MSI scores for 499 independent replicates of two MSS and two MSI-H–contrived materials run across 499 separate sequencing runs. Dashed line indicates the sample-level threshold for MSI detection.

in detection efficiency thereafter. As such, samples with a circulating tumor fraction (as defined by the maximum somatic variant allele fraction) of <0.2% were considered unevaluable for MSI status.

Analytical validation studies

To assess the analytical sensitivity of MSI detection, cfDNA derived from the supernatant of the MSI-H cell line KM12 was diluted into MSS cfDNA targeting five titration points comprising 15 independently processed replicates bracketing the LoD predicted by the *in silico* simulations described above. Each

titration series was analyzed at both 5 ng, the minimum acceptable cfDNA input, and 30 ng, the maximum and most common cfDNA input. Using probit analysis, the 95% LoD (LOD_{95}) was calculated to be 0.4% at 5-ng input (Fig. 2A) and 0.1% at 30-ng input (Fig. 2B).

To assess analytical intermediate precision, we analyzed replicates of four different contrived materials, two MSS and two MSI-H (Fig. 2C). Across 499 replicates, categorical concordance for MSI status was 100% (499/499, 95% CI, 99%–100%), with coefficients of variation for quantitative MSI score ranging from 6.3%–7.2% for MSI-H samples (Supplementary Table 1). Repeatability and input robustness were also assessed by replicate testing of MSS and MSI-H–contrived material at 5-, 10-, and 30-ng cfDNA input, which similarly demonstrated 100% concordance (27/27, 95% CI, 85%–100%, Supplementary Fig. S1; Supplementary Table S2). Clinical precision was confirmed in 72 independent patient sample replicates representing a range of MSI scores and tumor fractions processed across three independent batches, days, operators, and reagent lots, which demonstrated a qualitative concordance of 100% (72/72, 95% CI, 94%–100%) with coefficients of variation for the underlying quantitative MSI score of 2.0%–15.2% (Supplementary Table S3).

To assess analytical specificity, healthy donor plasma samples (distinct from those used in training), MSS-contrived materials, and MSS patient samples were analyzed for spurious MSI-H calls. Analytical specificity was 100% across healthy donor samples (20/20, 95% CI, 83%–100%), contrived material (245/245, 95% CI, 98%–100%), and patient samples (48/48, 95% CI, 92%–100%).

Clinical validation studies

As no orthogonal cfDNA-based method was available to use as a comparator, clinical accuracy was determined by comparing ctDNA MSI assessment to MSI status from the medical record determined using standard-of-care tissue testing (a mixture of IHC, PCR, and NGS methods) for 1,145 samples comprising 40 distinct cancer types, 15 of which had at least five representative specimens (Supplementary Fig. S2). In 949 unique evaluable patients, ctDNA detected 87% of patients reported as MSI-H (71/82, 95% CI, 77%–93%) and 99.5% of patients reported as MSS/MSI-L (863/867, 95% CI, 98.7%–99.8%) for an overall accuracy of 98.4% (934/949, 95% CI, 97.3%–99.1%), with a positive predictive value (PPV) of 95% (71/75, 95% CI, 86%–98%; Fig. 3A; Supplementary Table S4). Consistent with *in silico* modeling studies, MSI-H detection was rare (0/19) in samples classified as unevaluable due to low tumor fraction (Fig. 3B), which explained 57% (16/28) of the observed ctDNA-tissue discordance in the total unique patient sample set (Supplementary Table S4). For samples with tumor fractions above 1%, ctDNA PPA rose to 93% (54/58, 95% CI, 82%–98%, Supplementary Table S4D).

Interestingly, despite the high correlation between IHC and PCR tissue tests reported in the literature (22, 35), concordance between ctDNA and tissue MSI status here varied by tissue test methodology [97.4% by PCR (450/462), 98.0% by NGS (239/244), and 83.0% by IHC (93/112), Fig. 3C; Supplementary Table S5]. On further investigation, it was noted that this discordance was due to both an increased tissue IHC-positive, ctDNA-negative population (2.4% by PCR, 2.0% by NGS, and 12.5% by IHC, Fisher exact test $P < 0.001$ for IHC-PCR and IHC-NGS) and an increased tissue IHC-negative, ctDNA-positive population
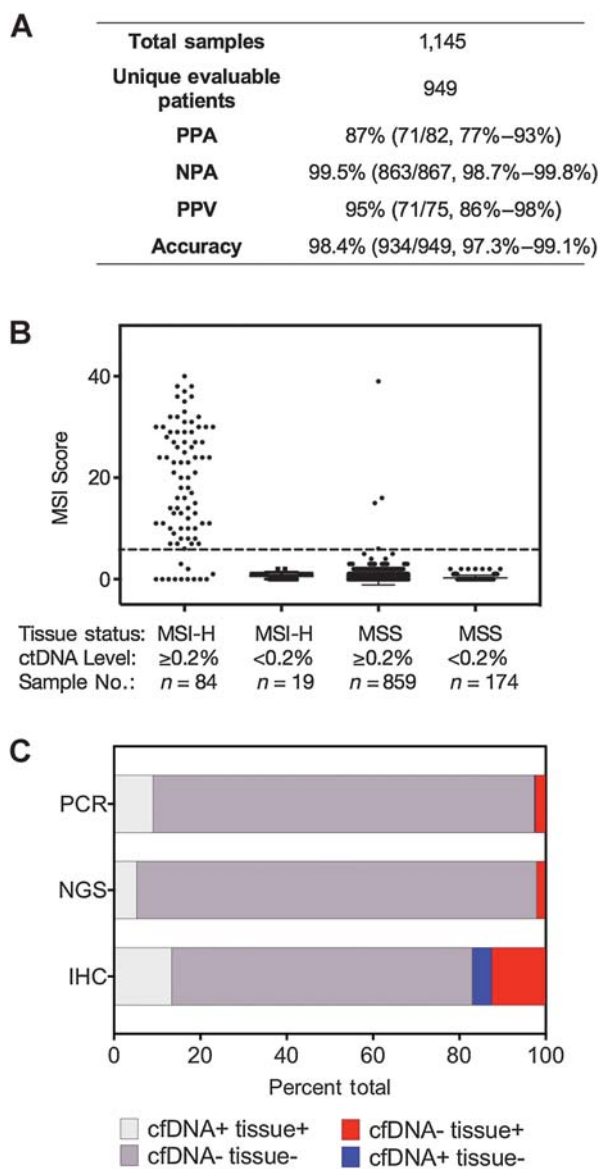
Figure 3.
Concordance of ctDNA MSI status with tissue testing. **A,** Sample-level MSI scores for 1,145 cfDNA samples categorized by tissue test result and observed tumor fraction. Dashed line indicates the sample-level threshold for MSI detection. **B,** Concordance result categorized by tissue test methodology. **C,** Descriptive statistics for the evaluable unique patient cohort are presented with absolute count and 95% CIs in parentheses.

(0.2% by PCR, 0% by NGS, and 4.5% by IHC, Fisher exact test $P < 0.01$ for both comparisons). Of the 25 samples for which IHC and another tissue test results were available, 12 demonstrated IHC-ctDNA discordance. Importantly, PCR and/or NGS tissue testing supported the ctDNA NGS results rather than the tissue IHC in 5 of 12 discordances, indicating that the discordance observed between ctDNA NGS and tissue IHC in this cohort was, at least, partially due to IHC-derived factors rather than solely ctDNA-tissue discordance. Together, these data suggest that ctDNA assessment may provide a valuable corroborative method for MSI assessment.

## ctDNA MSI status in 28,459 patient samples with consecutive advanced cancer

Although a number of studies have assessed the prevalence of MSI across different tumor types in tissue (13, 28, 36), to date there is no published landscape analysis of ctDNA MSI status across cancer types. To this end, we applied the MSI algorithm described above to 28,459 consecutive advanced cancer patient clinical samples tested in the Guardant Health Clinical Laboratory. In this cohort, 278 samples (tumor fraction median of 6.55%, range 0.09%–89%) comprising 16 different tumor types were identified as MSI-H by ctDNA, which corresponds to an overall pan-cancer prevalence of approximately 1%, similar to that previously reported for tissue (13, 28, 36). Similarly, MSI-H prevalence among tumor types also closely reflected that observed in tissue-based analyses (Fig. 4A); as expected, MSI-H was most prevalent in endometrial, colorectal, and gastric cancers, whereas other tumors such as lung, bladder, and head and neck cancers demonstrated lower prevalence. Specific exceptions to previous MSI-H prevalence estimates included marginally lower prevalence in endometrial, colorectal, and gastric cancers, and marginally higher prevalence in prostate cancer.

Given the pan-solid tumor nature of the ctDNA intended use population and immunotherapy approval for MSI-H tumors, microsatellite loci for this panel were intentionally selected to be informative of MSI status across all solid tumor types. Consistent with this design intent, analysis of sample- and locus-level MSI score distributions (Fig. 4B and C) demonstrated consistent performance across tumor types, with MSI-H samples demonstrating signal substantially above threshold. Moreover, the diagnostic yield of MSI assessment outside of the tumor types for which MSI is commonly tested was substantial; more than half of the identified cases (143/278) occurred in tumor types in which MSI testing is very uncommon (Fig. 4A) and thus identified patients that would otherwise never have been tested.

Consistent with what has been reported in tissue (13), the number of indels and SNVs (inclusive of nonsynonymous and synonymous variants) is significantly increased in MSI-H samples relative to those characterized as having MSS status (Fig. 5). Specifically, the median number of SNVs in MSI-H samples was 6.3 versus 1.4 in MSS (χ^2 $P < 0.0001$) and the median number of indels in MSI-H samples was 2.6 versus 0.4 in MSS (χ^2 $P < 0.0001$).

ctDNA MSI status predicts immunotherapy response

The most salient utility of MSI status today is its ability to select patients for immunotherapy. Despite this and the barriers to obtaining tissue in many patients, the ability of ctDNA MSI status to predict response to immunotherapy has not been reported. To establish clinical validity for this biomarker, we present clinical outcomes for 16 patients with ctDNA MSI-H metastatic gastric cancer treated with pembrolizumab ($n = 15$) or nivolumab ($n = 1$) after the failure of standard-of-care chemotherapy in a phase II pembrolizumab trial in gastric cancer (NCT#02589496). cfDNA and tissue PCR MSI assessment in pretreatment samples was 100% concordant for MSI-H (16/16, 95% CI, 76%–100%). Ten of 16 patients achieved either complete ($n = 3$) or partial ($n = 7$) investigator-assessed objective response by RECIST 1.1 criteria, with an additional three patients with stable disease (Fig. 6A), for
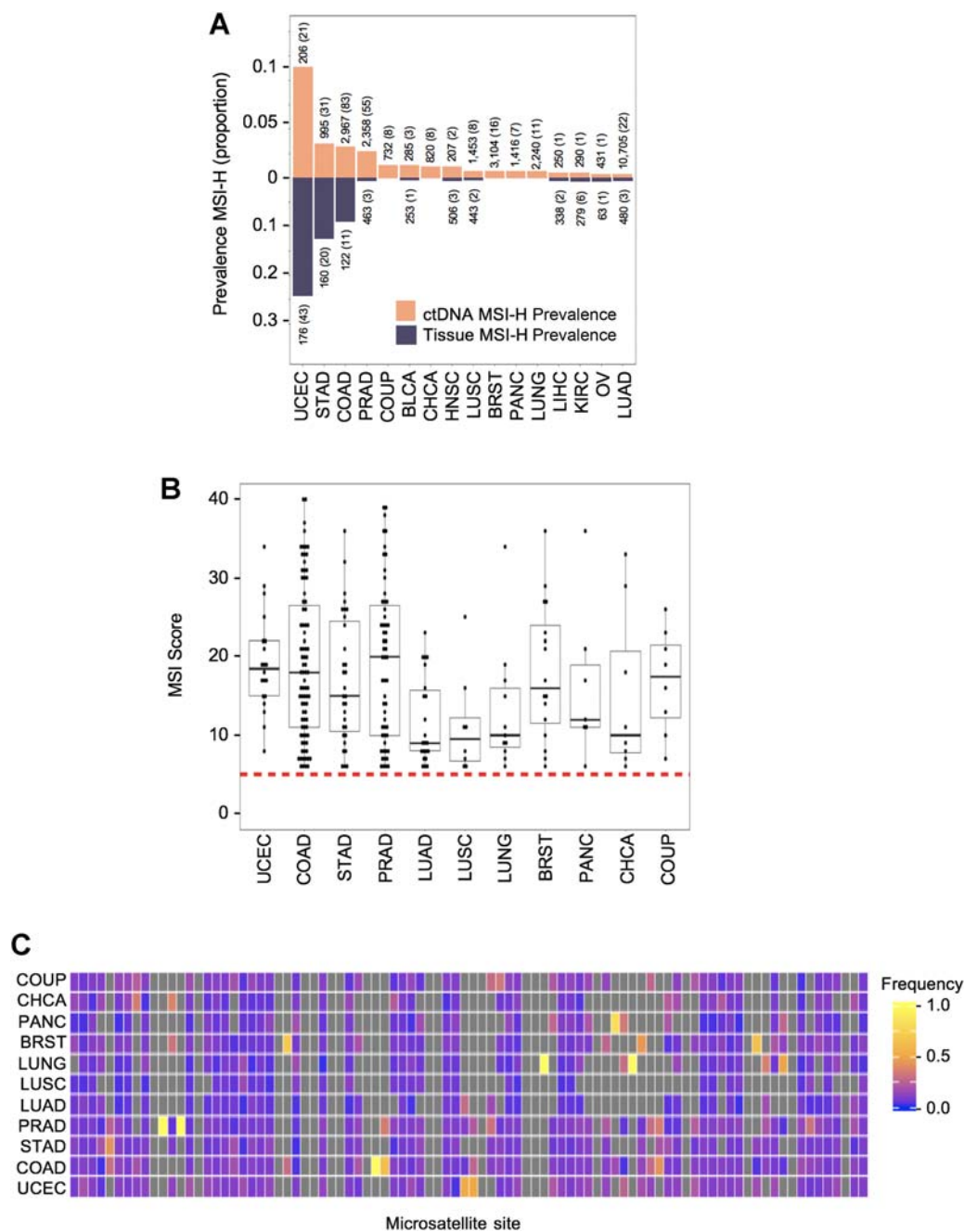
Figure 4.
ctDNA MSI landscape across 28,459 clinical samples. **A,** Positive axis reports ctDNA MSI prevalence across 16 most prevalent tumor types in the sample set. Negative axis reports the tissue MSI prevalence across the same based on Hause and colleagues (32). The total number of samples are reported above each with the number of MSI-H samples in parentheses. **B,** Sample-level MSI scores by tumor type for tumor types with ≥ 5 MSI-H samples. Dashed line indicates the sample-level threshold for MSI detection. **C,** Frequency of individual microsatellite sites contributing to MSI-H samples by tumor type for tumor types with ≥ 5 MSI-H samples. UCEC, uterine corpus endometrial carcinoma; STAD, stomach adenocarcinoma; COAD, colon adenocarcinoma; PRAD, prostate adenocarcinoma; COUP, cancer of unknown primary; BLCA, bladder carcinoma; CHCA, cholangiocarcinoma; HNSC, head and neck squamous cell carcinoma; LUSC, lung squamous cell carcinoma; BRST, breast carcinoma; PANC, pancreatic adenocarcinoma; LUNG, lung cancer, not otherwise specified; LIHC, liver hepatocellular carcinoma; KIRC, kidney renal cell carcinoma; OV ovarian carcinoma; LUAD, lung adenocarcinoma.

an objective response rate of 63% (10/16, 95% CI, 36%–84%) and a disease control rate of 81% (13/16, 95% CI, 54%–95%), similar to responses previously reported for MSI-H patients defined by tissue testing (37). Importantly, even in this pretreated population, these responses were durable, with a median duration of treatment of 39 weeks. Indeed, patient 21, for example, experienced complete regression of disease following pembrolizumab treatment after failure of fluoropyrimidine/platinum
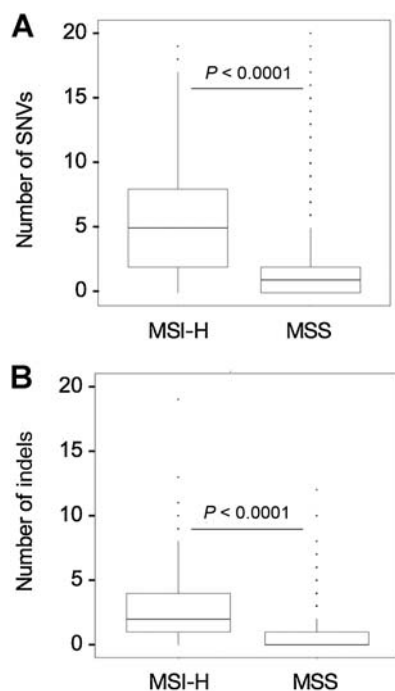
Figure 5.
Tumor mutation burden by MSI status. Number of SNVs (**A**) and indels (**B**) detected per sample categorized by MSI status across 278 MSI-H and 28,181 MSS samples.

chemotherapy and is still disease-free more than 6 months following completion of 35 cycles of therapy (Fig. 6B–E).

Discussion

We have validated a novel cfDNA-based targeted NGS approach for MSI detection. By using a large panel of microsatellite loci, this approach achieved high sensitivity relative to tissue-based methods, while maintaining very high specificity. Plasma-detected prevalence of MSI-H across 16 common solid tumors was similar to published tissue-based compendia, compatible with the intended pan-cancer design of the sequencing panel and MSI detection algorithm. Furthermore, we demonstrate clinical utility by showing that MSI-H patients as detected by cfDNA benefit from ICB therapy in a manner similar to that reported for tissue-defined populations (37), expanding the availability of MSI detection to all patients regardless of tissue availability or requirement to undergo invasive tissue acquisition procedures.

This study demonstrates robust analytic performance for MSI detection on a cfDNA panel previously validated for detection of the other four variant types in all guideline-recommended indications (25). In particular, the analytic sensitivity for MSI detection in contrived samples demonstrated reproducible detection to 0.1%, congruent with previous reports of similar sensitivity for indels and SNVs (25). Importantly, this study assessed the performance of ctDNA MSI testing in 1,145 samples with orthogonal tissue MSI, which constitutes the largest ctDNA-tissue MSI concordance cohort yet described. Relative to standard-of-care tissue MSI testing for the same patients, ctDNA MSI assessment demonstrated high PPV (95%), which

compares favorably to the reported PPV of 90%–92% reported for local versus central tissue–based MSI assessment (38), and high PPA (87%) in the evaluable population, which is consistent with previous studies examining concordance of plasma and tissue genotyping for other variant types (24, 25, 39, 40). Factors that can contribute to incomplete concordance may include tumor heterogeneity, differential shedding by the primary versus metastatic lesions, temporal discordance of tissue and plasma collection, and low tumor shedding by some tumors (41–45). Interestingly, a patient with gastric cancer identified as MSI-H by plasma and by pentaplex PCR in this report was previously reported to comprise discrete tumor populations of MSS and MSI-H disease as assessed by both IHC and PCR performed on tissue (41). The same study found 9% discordance for MSI-H between paired tissue biopsies in the same patient (41), highlighting the potential contribution of intratumoral heterogeneity to discordances in MSI status. Moreover, the observation of nontrivial discordance between PCR and IHC tissue methods in this report highlight the importance of accurate MSI testing, which has been reported as a primary source of ICB failure (38). Consistent with the challenges presented by tissue genotyping in advanced solid tumors, a study in metastatic non–small cell lung cancer has shown that relative to tissue, plasma-based testing increases the number of patients with successful tumor genotyping results, as well as the frequency of detecting targetable mutations (24, 39).

This study presents the first ctDNA-based landscape analysis of MSI in a large advanced pan-cancer cohort. Overall, the relative prevalence across tumor types in a set of >28,000 consecutive clinical samples are consistent with what has been reported for tissue (13, 28, 36), with only marginal differences. For example, the prevalence in colorectal cancer and endometrial cancer is lower than what has been reported for tissue (13), which most likely reflects the fact that tissue-based landscape analyses include large numbers of early-stage MSI-H tumors, which have a better prognosis (15) and are less likely to be part of the advanced cancer population tested with ctDNA. In contrast, the larger than expected prevalence of MSI-H prostate cancer is attributable to increased representation of MSI-H disease in advanced patients; two recent studies focusing on MSI status in advanced prostate cancer have shown MSI-H prevalence of 3.1% and 3.8% in that patient population (46, 47), which is similar to the 2.6% observed in this study. Unsurprisingly, given the design intent for pan-cancer MSI detection, landscape analysis did not reveal tumor type–specific patterns of microsatellite instability. This design approach allows standardization of MSI detection across tumor types, including those without available training sets; however, it does not preclude the possibility that in plasma, similar to what has been shown in tissue (28, 36), tumor-type–specific patterns could emerge with the assessment of larger numbers of representative MSI-H samples or larger numbers of microsatellite loci.

The clinical outcomes reported here are limited to gastric cancer; nevertheless, the observed objective response rate is consistent with expectations from tissue-based studies, suggesting that ICB treatment based on cfDNA MSI results should achieve expected outcomes across solid tumor types. In addition, lack of germline dMMR data prevented conclusions about familial implications for cfDNA-detected MSI; however, while cfDNA-detected MSI may raise suspicion for hereditary cancer predisposition syndromes, the test's 87% PPA relative to tissue-
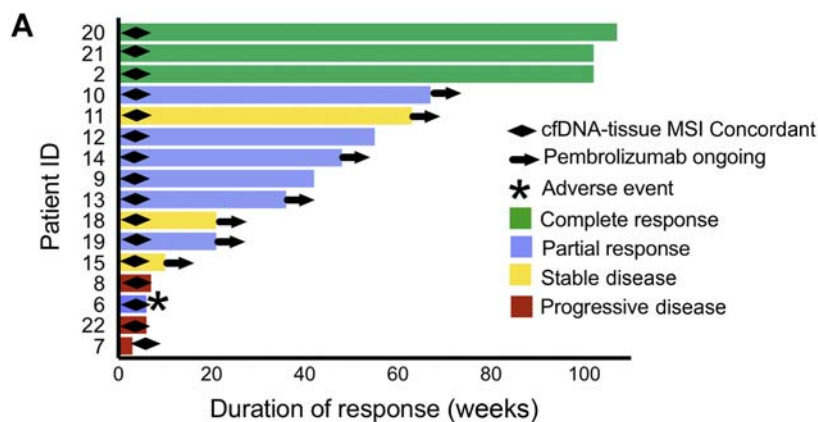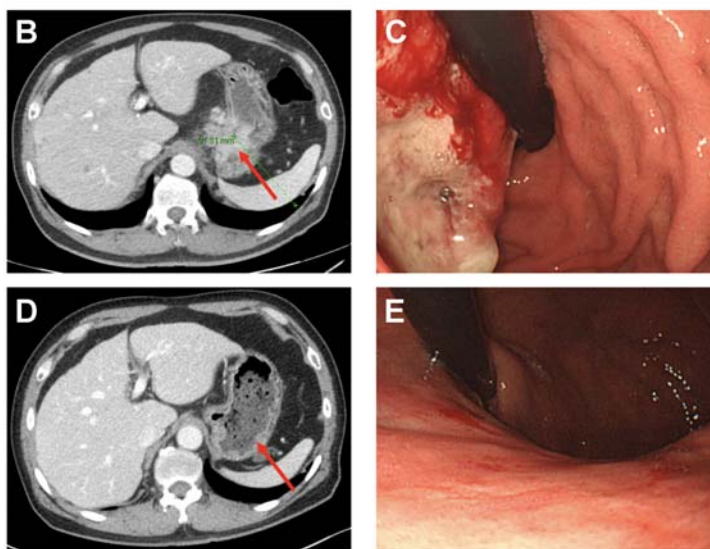
Figure 6.
Clinical outcome to ICB therapy in ctDNA MSI-H patients. **A,** Swimmer plot of duration of ICB therapy in months. Baseline (**B** and **C**) and post-therapy (**D** and **E**) CT (**B** and **D**) and gastroendoscopy (**C** and **E**) for patient 21.

based testing precludes its use as a screening test for these conditions. Finally, treatment data were not available for the majority of patients with cfDNA-/tissue+ discordance, but it is expected that at least some have received ICB therapy based on the tumor result, which would suppress MSI-H disease and lead to lack of MSI detection by cfDNA, thereby contributing to the observed discordance. Future studies should be pursued to address these questions.

In summary, we have developed and validated a cfDNA-based targeted NGS panel that accurately assesses MSI status while also providing comprehensive tumor genotyping, allowing pan-solid tumor guideline-complete testing from a single peripheral blood draw with high sensitivity, specificity, and precision. Clinical validation using both comparison to tissue testing, population-level prevalence analyses, and the first-reported outcomes for cfDNA MSI-H patients treated with ICB therapy supported the clinical accuracy and relevance of this approach. Such simultaneous characterization of MSI status and tumor genotype from a simple peripheral blood draw has the potential to expand access to both targeted therapy and immunotherapies to all patients with advanced cancer including those for whom current tissue-based testing paradigms are inadequate.

Disclosure of Potential Conflicts of Interest

M.I. Lefterova holds ownership interest (including patents) in Guardant Health. D.V.T. Catenacci reports receiving speakers bureau honoraria from Guardant Health, Foundation Medicine, and Merck, and is a consultant/advisory board member for Merck and Bristol-Myers Squibb. M. Fakih reports receiving speakers bureau honoraria from Amgen, and is a consultant/advisory board member for Array, Seattle Genetics, and Amgen. D. Gavino holds ownership interest (including patents) in Guardant Health and Invitae. N. Peled reports receiving speakers bureau honoraria from and is a consultant/advisory board member for AstraZeneca, BI, Bristol-Myers Squibb, FoundationMedicine, Gaurdant, Lilly, MSD, Novartis, Pfizer, and Roche. R.N. Eskander reports receiving speakers bureau honoraria from AstraZeneca and Clovis Oncology, and is a consultant/advisory board member for Merck, Eisai, Pfizer, and Tesaro/GSK. G. Azzi holds ownership interest (including patents) in and reports receiving speakers bureau honoraria from Guardant Health. K.C. Banks, D.I. Chudova, and A. Talasaz hold ownership interest (including patents) in Guardant Health. R.B. Lanman is an employee of Guardant Health, Inc, holds ownership interest (including patents) in Guardant Health, Inc, Biolase, Inc, and Forward Medical, Inc, and is a consultant/advisory board member for Forward Medical, Inc and Biolase, Inc. No potential conflicts of interest were disclosed by the other authors.

Authors' Contributions

Conception and design: M.I. Lefterova, A. Artyomenko, P.M. Kasi, K. Mody, D.V.T. Catenacci, C. Barbacioru, D. Gavino, N. Peled, R.N. Eskander, K.C. Banks, V.M. Raymond, R.B. Lanman, D.I. Chudova, A. Talasaz, J.I. Odegaard

References

1. Koh W-J, Abu-Rustum NR, Bean S, Bradley K, Campos SM, Cho KR, et al. Cervical cancer, version 3.2019, NCCN Clinical Practice Guidelines in Oncology. J Natl Compr Canc Netw 2019;17:64–84.
2. Benson Al B, D'Angelica MI, Abbott DE, Abrams TA, Alberts SR, Anaya DA, et al. Hepatobiliary cancers, version 4.2018: featured updates to the NCCN guidelines; 2018. Available from: https://www.nccn.org/professionals/physician_gls/pdf/hepatobiliary.pdf.
3. Benson Al B, Venook AP, Bekaii-Saab T, Chan E, Chen YJ, Cooper HS, et al. Colon cancer version 1.2016, NCCN Practice Guidelines in Oncology; 2015. Available from: https://www.nccn.org/professionals/physician_gls/pdf/colorectal.pdf.
4. Koh W-J, Abu-Rustum NR, Bean S, Bradley K, Campos SM, Cho KR, et al. Uterine neoplasms, version 1.2018, NCCN Clinical Practice Guidelines in Oncology. J Natl Compr Canc Netw 2018;16:170–99.
5. Ajani JA, D'Amico TA, Baggstrom M, Bentrem DJ, Chao J, Das P, et al. Esophageal and esophagogastric junction cancers version 4.2017; 2017. Available from: https://www.nccn.org/professionals/physician_gls/pdf/esophageal.pdf.
6. Ajani JA, D'Amico TA, Baggstrom M, Bentrem DJ, Chao J, Das P, et al. Gastric cancer, version 5.2017, NCCN Clinical Practice Guidelines in Oncology; 2017. Available from: https://www.nccn.org/professionals/physician_gls/pdf/gastric.pdf.
7. Armstrong DK, Alvarez RD, Bakkum-Gamez JN, Barroilhet L, Behbakht K, Berchuck A, et al. NCCN guidelines version 1.2019 ovarian cancer; 2019. Available from: https://www.nccn.org/professionals/physician_gls/pdf/ovarian.pdf.
8. Tempero MA, Malafa MP, Al-Hawary M, Asbun H, Bain A, Behrman SW, et al. Pancreatic adenocarcinoma version 2.2018, NCCN Clinical Practice Guidelines in Oncology; 2018. Available from: https://www.nccn.org/professionals/physician_gls/pdf/pancreatic.pdf.
9. Mohler JL, Lee RJ, Antonarakis ES, Armstrong AJ, D'Amico AV, Davis BJ, et al. NCCN guidelines version 1.2018 prostate cancer; 2018. Available from: https://www.nccn.org.
10. Diaz LA, Le DT. PD-1 blockade in tumors with mismatch-repair deficiency. N Engl J Med 2015;373:1979.
11. Le DT, Durham JN, Smith KN, Wang H, Bartlett BR, Aulakh LK, et al. Mismatch-repair deficiency predicts response of solid tumors to PD-1 blockade. Science 2017;357:409–13.
12. Buza N, Ziai J, Hui P. Mismatch repair deficiency testing in clinical practice. Expert Rev Mol Diagn 2016;16:591–604.
13. Bonneville R, Krook MA, Kautto EA, et al. Landscape of microsatellite instability across 39 cancer types. JCO Precis Oncol 2017;2017:10.1200/PO.17.00073. doi:10.1200/PO.17.00073.
14. Marcus L, Lemery SJ, Keegan P, Pazdur R. FDA approval summary: pembrolizumab for the treatment of microsatellite instability-high solid tumors. Clin Cancer Res 2019;25:3753–8.
15. Benson AB, Arnoletti JP, Bekaii-Saab T, Chan E, Chen Y-J, Choti MA, et al. Colon cancer. J Natl Compr Canc Netw 2011;9:1238–90.
16. Boland CR, Thibodeau SN, Hamilton SR, Sidransky D, Eshleman JR, Burt RW, et al. A National Cancer Institute Workshop on Microsatellite Instability for cancer detection and familial predisposition: development of international criteria for the determination of microsatellite instability in colorectal cancer. Cancer Res 1998;58:5248–57.
17. Umar A, Boland CR, Terdiman JP, Syngal S, de la Chapelle A, Rüschoff J, et al. Revised Bethesda Guidelines for hereditary nonpolyposis colorectal cancer (Lynch syndrome) and microsatellite instability. J Natl Cancer Inst 2004;96:261–8.
18. Lu Y, Soong TD, Elemento O. A novel approach for characterizing microsatellite instability in cancer cells. PLoS One 2013;8:e63056.
19. Dudley JC, Lin M-T, Le DT, Eshleman JR. Microsatellite instability as a biomarker for PD-1 blockade. Clin Cancer Res 2016;22:813–20.
20. Salipante SJ, Scroggins SM, Hampel HL, Turner EH, Pritchard CC. Microsatellite instability detection by next generation sequencing. Clin Chem 2014;60:1192–9.
21. Latham A, Srinivasan P, Kemel Y, Shia J, Bandlamudi C, Mandelker D, et al. Microsatellite instability is associated with the presence of lynch syndrome pan-cancer. J Clin Oncol 2019;37:286–95.
22. Hampel H, Frankel WL, Martin E, Arnold M, Khanduja K, Kuebler P, et al. Screening for the Lynch syndrome (hereditary nonpolyposis colorectal cancer). N Engl J Med 2005;352:1851–60.
23. Shaikh T, Handorf EA, Meyer JE, Hall MJ, Esnaola NF. Mismatch repair deficiency testing in patients with colorectal cancer and non-adherence to testing guidelines in young adults. JAMA Oncol 2017;4:e173580.
24. Leighl NB, Page RD, Raymond VM, Daniel DB, Divers SG, Reckamp KL, et al. Clinical utility of comprehensive cell-free DNA analysis to identify genomic biomarkers in patients with newly diagnosed metastatic non-small cell lung cancer. Clin Cancer Res 2019 Apr 15. doi: 10.1158/1078-0432.CCR-19-0624. [Epub ahead of print.].
25. Odegaard JI, Vincent JJ, Mortimer S, Vowles JV, Ulrich BC, Banks KC, et al. Validation of a plasma-based comprehensive cancer genotyping assay utilizing orthogonal tissue- and plasma-based methodologies. Clin Cancer Res 2018;24:3539–49.
26. Lanman RB, Mortimer SA, Zill OA, Sebisanovic D, Lopez R, Blau S, et al. Analytical and clinical validation of a digital sequencing panel for quantitative, highly accurate evaluation of cell-free circulating tumor DNA. PLoS One 2015;10:e0140712.
27. Akaike H. Information Theory and an Extension of the Maximum Likelihood Principle. In: Parzen E, Tanabe K, Kitagawa G, eds. Selected Papers of Hirotugu Akaike. Springer Series in Statistics (Perspectives in Statistics). New York, NY: Springer; 1998.

28. Hause RJ, Pritchard CC, Shendure J, Salipante SJ. Classification and characterization of microsatellite instability across 18 cancer types. Nat Med 2016;22:1342–50.

29. Characterization of the cell-free DNA released by cultured cancer cells. Biochim Biophys Acta 2016;1863:157–65.

30. Berg KCG, Eide PW, Eilertsen IA, Johannessen B, Bruun J, Danielsen SA, et al. Multi-omics of 34 colorectal cancer cell lines - a resource for biomedical studies. Mol Cancer 2017;16:116.

31. Catalogue of Somatic Mutations in Cancer. COSMIC - Catalogue of Somatic Mutations in Cancer. Available from: https://cancer.sanger.ac.uk/cosmic.

32. Forbes SA, Beare D, Boutselakis H, Bamford S, Bindal N, Tate J, et al. COSMIC: somatic cancer genetics at high-resolution. Nucleic Acids Research 2017;45:D777–83.

33. Georgiadis A, Wood D, Murphy D, Parpart-Li S, Riley D, Sengamalay N, et al. Abstract 1286: analytical validation of an integrated next-generation sequencing pan-cancer liquid biopsy approach for detection of microsatellite instability. Cancer Res 2018;78:1286.

34. Zill OA, Banks KC, Fairclough SR, Mortimer SA, Vowles JV, Mokhtari R, et al. The landscape of actionable genomic alterations in cell-free circulating tumor DNA from 21,807 advanced cancer patients. Clin Cancer Res 2018;24:3528–38.

35. Lindor NM, Burgart LJ, Leontovich O, Goldberg RM, Cunningham JM, Sargent DJ, et al. Immunohistochemistry versus microsatellite instability testing in phenotyping colorectal tumors. J Clin Oncol 2002;20: 1043–8.

36. Vanderwalde A, Spetzler D, Xiao N, Gatalica Z, Marshall J. Microsatellite instability status determined by next-generation sequencing and compared with PD-L1 and tumor mutational burden in 11,348 patients. Cancer Med 2018;7:746–56.

37. Le DT, Uram JN, Wang H, Bartlett BR, Kemberling H, Eyring AD, et al. PD-1 blockade in tumors with mismatch-repair deficiency. N Engl J Med 2015; 372:2509–20.

38. Cohen R, Hain E, Buhard O, Guilloux A, Bardier A, Kaci R, et al. Association of primary resistance to immune checkpoint inhibitors in metastatic colorectal cancer with misdiagnosis of microsatellite instability or mismatch repair deficiency status. JAMA Oncol 2019;5:551.

39. Aggarwal C, Thompson JC, Black TA, Katz SI, Fan R, Yee SS, et al. Clinical implications of plasma-based genotyping with the delivery of personalized therapy in metastatic non-small cell lung cancer. JAMA Oncol 2018 Oct 12 [Epub ahead of print].

40. Siravegna G, Lazzari L, Crisafulli G, Sartore-Bianchi A, Mussolin B, Cassingena A, et al. Radiologic and genomic evolution of individual metastases during HER2 blockade in colorectal cancer. Cancer Cell 2018;34: 148–162.

41. Kim ST, Cristescu R, Bass AJ, Kim K-M, Odegaard JI, Kim K, et al. Comprehensive molecular characterization of clinical responses to PD-1 inhibition in metastatic gastric cancer. Nat Med 2018;24: 1449–58.

42. Goyal L, Saha SK, Liu LY, Siravegna G, Leshchiner I, Ahronian LG, et al. Polyclonal secondary FGFR2 mutations drive acquired resistance to FGFR inhibition in patients with FGFR2 fusion-positive cholangiocarcinoma. Cancer Discov 2017;7:1–12.

43. Pectasides E, Stachler MD, Derks S, Liu Y, Maron S, Islam M, et al. Genomic heterogeneity as a barrier to precision medicine in gastroesophageal adenocarcinoma. Cancer Discov 2018;8:37–48.

44. Thompson JC, Yee SS, Troxel AB, Savitch SL, Fan R, Balli D, et al. Detection of therapeutically targetable driver and resistance mutations in lung cancer patients by next-generation sequencing of cell-free circulating tumor DNA. Clin Cancer Res 2016;22: 5772–82.

45. Sacher AG, Komatsubara KM, Oxnard GR. Application of plasma genotyping technologies in non-small cell lung cancer: a practical review. J Thorac Oncol 2017;12:1344–56.

46. Mayrhofer M, De Laere B, Whitington T, Van Oyen P, Ghysel C, Ampe J, et al. Cell-free DNA profiling of metastatic prostate cancer reveals microsatellite instability, structural rearrangements and clonal hematopoiesis. Genome Med 2018;10:85.

47. Abida W, Armenia J, Gopalan A, Brennan R, Walsh M, Barron D, et al. Prospective genomic profiling of prostate cancer across disease states reveals germline and somatic alterations that may affect clinical decision making. JCO Precis Oncol 2017 Jul. doi: 10.1200/PO.17.00029. Epub May 31, 2017.

AACR American Association
for Cancer Research

Clinical Cancer Research

Validation of Microsatellite Instability Detection Using a Comprehensive Plasma-Based Genotyping Panel

Jason Willis, Martina I. Lefterova, Alexander Artyomenko, et al.

Updated version	Access the most recent version of this article at: doi:10.1158/1078-0432.CCR-19-1324

E-mail alerts	Sign up to receive free email-alerts related to this article or journal.
Reprints and Subscriptions	To order reprints of this article or to subscribe to the journal, contact the AACR Publications Department at pubs@aacr.org.
Permissions	To request permission to re-use all or part of this article, use this link http://clincancerres.aacrjournals.org/content/early/2019/08/02/1078-0432.CCR-19-1324. Click on "Request Permissions" which will take you to the Copyright Clearance Center's (CCC) Rightslink site.